Imperial College London

Aerodynamic instability in a GT combustor operating with lean premixed H_2-enriched biogas blends

Siyi Qiu, Efstathios Karlis, Alex Taylor, Yannis Hardalupas

1. Introduction

1.1 Background:

- Biogas is a clean alternative for natural gas, as it produces zero carbon emission;
- Biogas can be further improved by hydrogen addition, in terms of its kinetic and dynamic characteristics.
- At lean premixed combustion mode, thermoacoustic oscillation is a major issue for gas turbine swirl combustors.

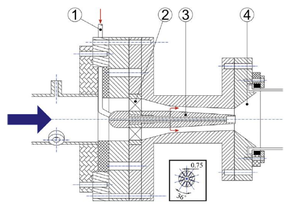

Fig.1. Sectional view of the swirl combustor: 1. fuel supply, 2. swirler, 3. centrebody, 4. diffuser

1.2 Research aim:

- To understand the contribution of aerodynamic instability to the onset of thermoacoustic oscillation for a hydrogen-enriched biogas fuel.

2. Method

2.1 Experimental technique:

High speed particle image velocimetry (PIV) to temporally resolve the unsteady flow field**.** Particles were illuminated by a 532nm Nd: YAG laser @3kHz. Field of view is 60×60mm^2@0.47mm/vector grid.

Dynamic pressure was sampled @20kHz as an indicator of acoustics by a microphone installed at the exhaust [1].

CH* chemiluminescence intensity signal was acquired @20kHz as an indicator of heat release rate by a photomultiplier [2].

2.2 Post processing & numerical technique:

Proper orthogonal decomposition (POD): to span PIV snapshots

$$u(\boldsymbol{x}, t_k) \approx \sum_{p=1}^{N} a_p(t_k)\Phi_p(\boldsymbol{x})$$

where $a_p(t_k)$ is the temporal coefficient and $\Phi_p(\boldsymbol{x})$ is the spatial POD mode.

Linear stability analysis (LSA): to solve the linear perturbation mode analytically. Perturbation is modelled as $u' = [\hat{u}; \hat{p}]\exp(i\varphi)$ and solved by the linearized N-S equation in cylindrical coordinates (r, θ, z)[3].

3. Aerodynamic instability

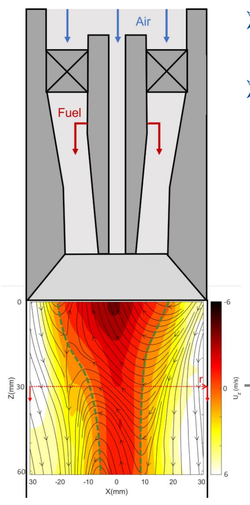

- The swirl combustor produces a confined swirling jet surrounding a recirculation zone.
- The base flow for stability analysis is the time-averaged isothermal velocity profile at z=30mm fitted by a modified Burgers vortex [4] with a 1/7th power law boundary layer to the wall.

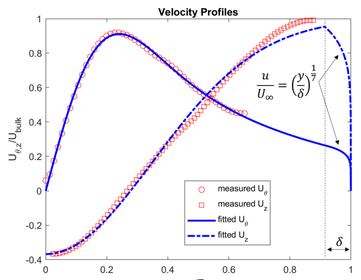

Fig.2. The time averaged flow field of the isothermal flow field in the combustor (left). Green dashed line shows the recirculation. The velocity profiles are then extracted and fitted by a modified Burgers vortex (right). The swirl velocity is measured from the cross-sectional plane at z=30mm.

- The dominating linear stability mode shows a helical velocity perturbation winding around the recirculation zone.
- Identical structure is also found in the most energetic POD mode.

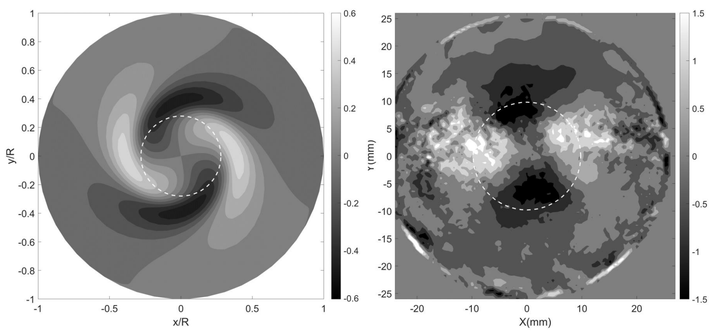

Fig.3. The dominating linear stability mode with azimuthal wavenumber of 2 (left) of the isothermal swirling jet. The domain is normalized by the radius of the combustor chamber R. The same structure is found in the most energetic POD mode extracted from cross-sectional measurement (left). The contours show the streamwise perturbation with arbitrary unit. The dotted circle denotes where U_z = 0.

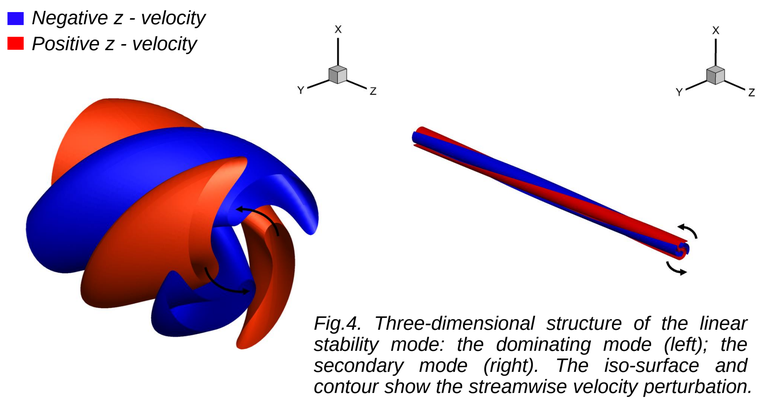

Fig.4. Three-dimensional structure of the linear stability mode: the dominating mode (left); the secondary mode (right). The iso-surface and contour show the streamwise velocity perturbation.

- Two discrete modes are found by the linear stability analysis: the dominating mode and the secondary mode.
- The dominating mode is unstable, as its growth rate is over zero; it is a helical perturbation (helical mode).
- The secondary mode is marginally stable, which localizes around, and close to, the centreline of the vortex (centre mode).
- The perturbation velocity undulates and generates a sequence of vortices. They perturbs the flow periodically when travelling downstream.
- It can be inferred that the PVC motion is induced by this helical perturbation mode.

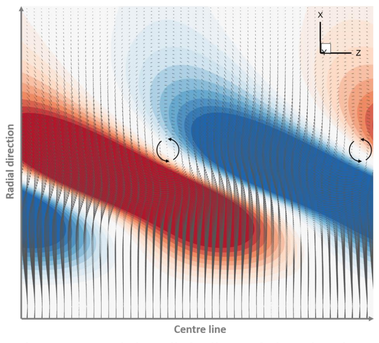

Fig.5. An axial-radial slice of the dominant linear stability mode, showing the propagation of vortical perturbation. The contour shows the streamwise velocity perturbation; the vectors show the in-plane velocity perturbation.

4. Dynamics of thermoacoustic oscillation

- The swirl combustor operates with three H2 molar concentrations (20%, 30% and 40%) in CH4 blends.
- The operation condition is selected so that the three cases are different in their dynamical states.

[c_{CH4}, c_{H2}]	Φ	Dynamic state	P_{th} (kW)
[80%, 20%]	0.55	Quiescent	33.10
[70%, 30%]	0.55	Intermittent	33.47
[60%, 40%]	0.55	Limit cycle	33.91

Tab.1 Experimental operation conditions.

4.1 Quiescent case (fig.6)

- The mild frequency peak @180Hz of *p* is coincident with the frequency peak of the most energetic POD mode.
- The most energetic POD mode shows vortices at the peripheral of the recirculation zone.
- The dominant stability mode also shows vortices around the recirculation zone, which may induce the vortices as shown in the POD mode.

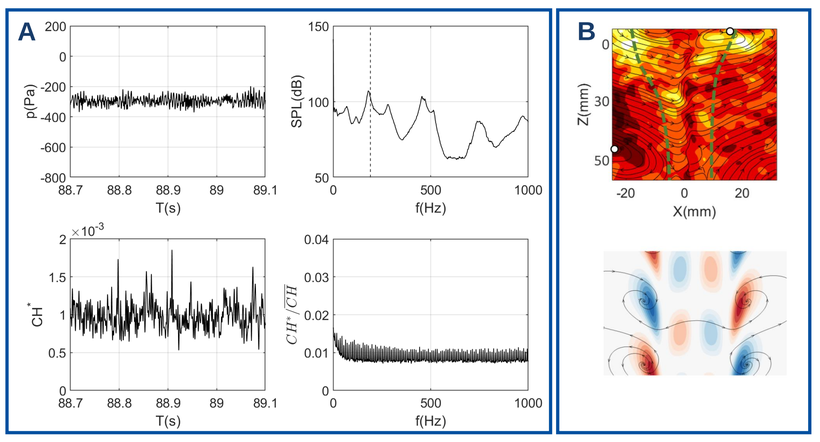

*Fig.6. (**A**)Time series (left column) and Fourier spectra (right column) of the dynamic pressure (top panel) and chemiluminescence intensity (bottom panel) for the quiescent case. The dashed line shows where the frequency peak of the most energetic POD mode (Mode 2) locates. (**B**) The most energetic POD mode (Mode 2) of the quiescent case (top) and the dominating linear stability mode (bottom) calculated from the isothermal swirl jet. Both modes show a vortex perturbation propagating downstream. Flow is from top to bottom in each figure. Contours in both figures show Y-vorticity. White dots show the location of the vortices; green dashed line shows the recirculation zone.*

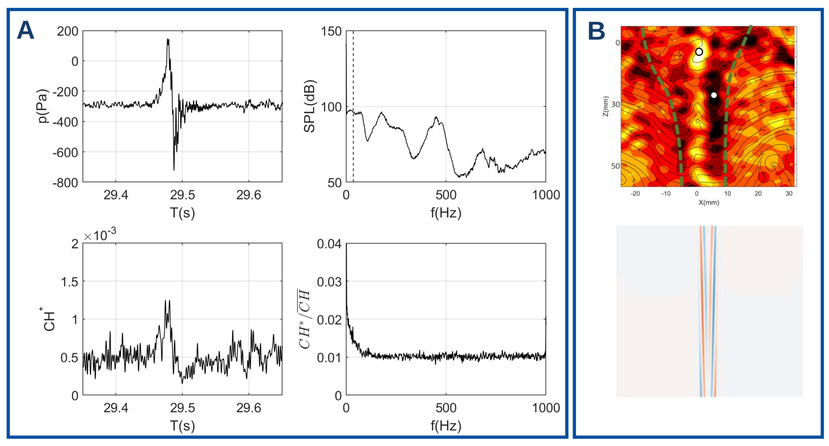

*Fig.7. (**A**) Same as fig.6 but for the intermittent case. The dashed line shows the location of the frequency peak of the most energetic POD mode (Mode 2) locates. (**B**) The most energetic POD mode (Mode 2) of the intermittent case (top) and the secondary linear stability mode (bottom) calculated from the isothermal swirl jet. Flow is from top to bottom in each figure. Contours in both figures show Y-vorticity.*

4.2 Intermittent case (fig.7)

- The most energetic POD mode reveals a ‘streak’ structure near the centerline.
- The ‘streak’ perturbation is similar in shape and location to that of the secondary, centre mode resolved by LSA (also in fig.4 right).

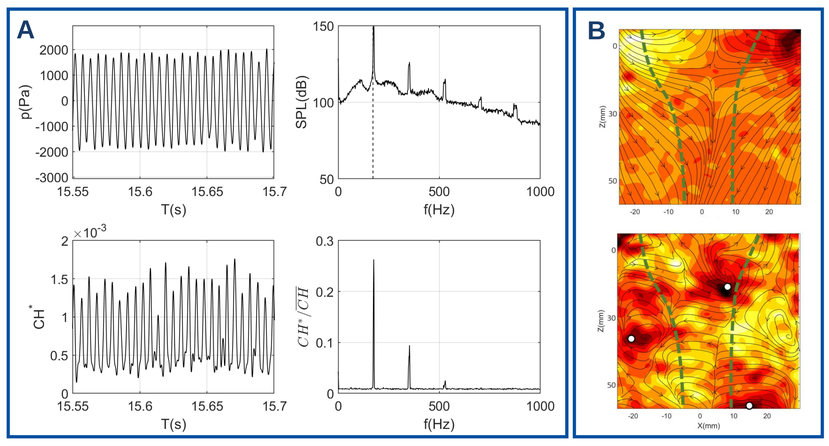

Fig. 8. (A) Same as fig.6 but for the limit-cycle case. The dashed line shows where the frequency peak of the most energetic POD mode (Mode 2) locates. (B) Limit-cycle case: the most energetic POD mode (Mode 2) (top) and Mode 13 showing propagating vortices (bottom). Flow is from top to bottom in each figure. Contours in both figures show Y-vorticity.

4.3 Limit-cycle case (fig.8)

- The case with c_{H2} = 40% goes into the limit cycle, where a large-amplitude, periodic oscillation can be observed in spectra for both the dynamic pressure and CH* intensity.
- Both Fourier spectra show a dominant frequency at 170Hz. This frequency is attributed to a ‘pumping’ mode, which periodically compresses and stretches the swirling jet.
- The vortex structures only become visible after the 13th mode. It can be inferred that PVC is suppressed in the limit cycle case.

5. Discussion & conclusion

The main findings of the present research are:

- The precessing vortex core (PVC) exists in the isothermal swirling jet in the swirl combustor. The PVC is attributed to a sequence of vortical perturbation propagating downstream.
- The helical mode, dominating in an isothermal condition, diminishes as the system goes from quiescence to limit cycle.
- A streak structure, resembling the secondary mode, dominates the transitioning mode to the limit cycle; its prevalence can be caused by transient effects. Future work will focus on the transient growth of this secondary mode.

Reference

[1] Karlis, E. (2019). Transient and Limit Cycle Thermoacoustic Oscillation Dynamics in a Lean Premixed Swirl Stabilized Combustor. PhD thesis, Imperial College London.

[2] Panoutsos, C. S., Hardalupas, Y., & Taylor, A. M. K. P. (2008). Effect of preheating on the local equivalence ratio at a swirl-stabilised partially-premixed combustor. 46th AIAA Aerospace Sciences Meeting and Exhibit.

[3] Khorrami, R. M., Malik, M. R., & Ash, R. L. (1989). Application of Spectral Collocation Techniques to the Stability of Swirling Flows. Journal of Computational Physics, 81, 206–229.

[4] Escudier, M. P., Bornstein, J., & Maxworthy, T. (1982). The dynamics of confined vortices. Proc. R. Soc. Lond, 360, 335–360.